High Enrichment of Heavy Metals in Fine Particulate Matter through Dust Aerosol Generation

Authors: Qianqian Gao[1, 2#], Shengqiang Zhu[1#], Kaili Zhou[1, 2], Jinghao Zhai[3], Shaodong Chen[1, 2], Qihuang Wang[1, 2], Shurong Wang[1], Jin Han[1, 2], Xiaohui Lu[1, 2], Hong Chen[1], Liwu Zhang[1, 2], Lin Wang[1, 2], Zimeng Wang[1, 2], Xin Yang[3], Qi Ying[4], Hongliang Zhang*[1], Jianmin Chen[1, 2]* and Xiaofei Wang*[1, 2]

[1]*Shanghai Key Laboratory of Atmospheric Particle Pollution and Prevention, Department of Environmental Science and Engineering, Fudan University, Shanghai 200433, China*

[2]*Shanghai Institute of Pollution Control and Ecological Security, Shanghai 200092, China*

[3]*School of Environmental Science and Engineering, Southern University of Science and Technology, Shenzhen 518055, China*

[4]*Zachry Department of Civil Engineering, Texas A&M University, College Station, TX 77843, USA*

Atmospheric Chemistry and Physics

Sep 4th, 2023

#These authors contributed equally to this paper

*To whom correspondence should be addressed.

Correspondence to:

Xiaofei Wang: Email: xiaofeiwang@fudan.edu.cn Tel: +86-021-31242526

Jianmin Chen: Email: jmchen@fudan.edu.cn Tel: +86(021)3124-2298

Hongliang Zhang: Email: zhanghl@fudan.edu.cn Tel: +86- 021-31248978

Abstract

Dust is a major source of atmospheric aerosols. Its chemical composition is often assumed to be similar to the parent soil. However, this assumption has not been rigorously verified. Here, we generated dust aerosols from soils to determine if there is particle size-dependent selectivity of heavy metals in the dust generation. Mn, Cd, Pb and other heavy metals were found to be highly enriched in fine ($PM_{2.5}$) dust aerosols, which can be up to ~6.5-fold. To calculate the contributions of dust to atmospheric heavy metals, regional air quality models usually use the dust chemical profiles from the US EPA's SPECIATE database, which does not capture the correct size-dependent selectivity of heavy metals in dust aerosols. Our air quality modeling for China demonstrates that the calculated contribution of fine dust aerosols to atmospheric heavy metals, as well as their cancer risks, could have significant errors without using proper dust profiles.

Graphical Abstract
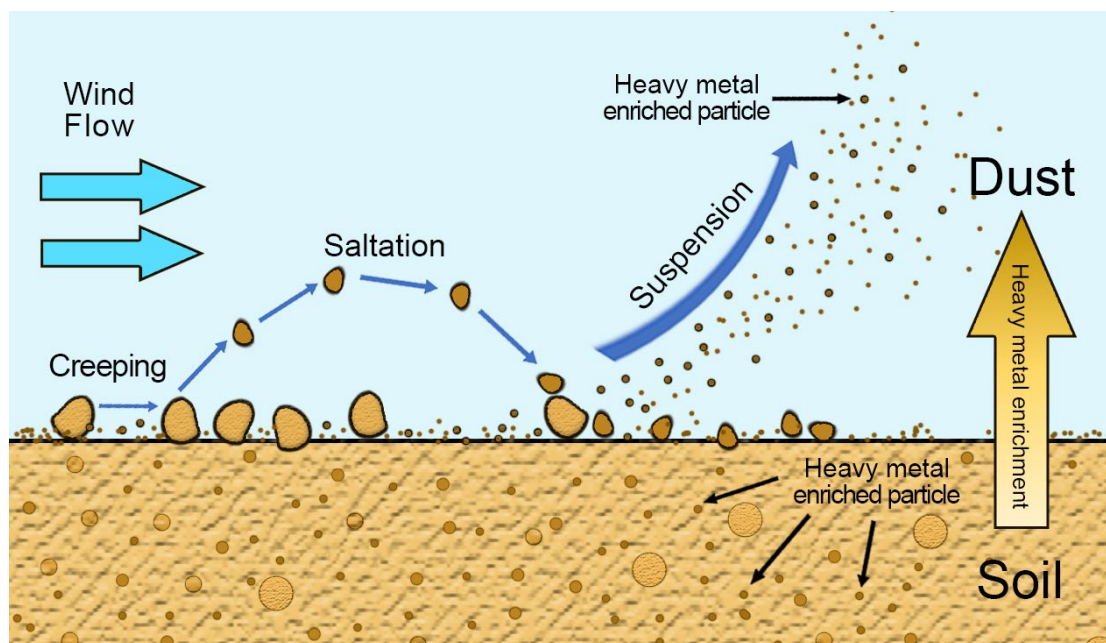
Short Summary

Dust is a major source of atmospheric aerosols. Its chemical composition is often assumed to be similar to the parent soil. However, this assumption has not been rigorously verified. Dust aerosols are mainly generated by wind erosion, which may have some chemical selectivity. Mn, Cd and Pb were found to be highly enriched in fine ($PM_{2.5}$) dust aerosols. In addition, estimation of heavy metal emission from dust generation by air quality models may have errors without using proper dust profiles.

1 Introduction

The major sources of natural aerosols include mineral dust aerosols produced by wind erosion (Prospero et al., 2002). Dust aerosols are influenced by regional atmospheric circulation, soil characteristics and local weather conditions (Bryant, 2013; Ding et al., 2005; Huebert et al., 2003; Liu et al., 2004; Yang et al., 2008), mainly generated and aerosolized when strong wind passes over soil or sandy areas (Gillette and Goodwin, 1974). Recent studies show mineral dust aerosol accounts for approximately 40% of the mass fraction of natural atmospheric aerosol, with an estimated annual flux of ~2,000 Tg·yr^{-1} (Alfaro, 2008; Griggs and Noguer, 2002; Huneeus et al., 2011; Textor et al., 2006). As the second-largest natural source of atmospheric aerosols in terms of mass flux, dust aerosol has a profound impact on the ecosystem (Middleton et al., 2019), especially the climate (Evan et al., 2014; Kok et al., 2018; Shao et al., 2013). Interactions between dust aerosols and water vapor play a critical role in cloud condensation and ice nucleation processes (Kaufman et al., 2002; Tang et al., 2016). Dust particles can be transported on large scales (Shao and Dong, 2006), and could act as a medium to transport toxic compounds, including heavy metals, which significantly harm human health, particularly the human respiratory system and even cause premature death (Urrutia-Pereira et al., 2021).

Atmospheric studies often assume that the chemical composition of aerosolized dust is similar to the parent soil (Gunawardana et al., 2012; Zhuang et al., 2001). The chemical composition of dust aerosol consists of a key part in source apportionment modeling (Balakrishna and Pervez, 2009; Samiksha et al., 2017; Santos et al., 2017; Ying et al., 2018). A critical approach in source apportionment modeling is the chemical transport model, which predicts the dust aerosol on global

72 and regional scales based on the prior knowledge of source emission, atmospheric transport, and

73 chemical reaction process. SPECIATE is the EPA's speciation profiles repository of air pollution

74 sources of volatile organic compounds (VOCs) and particulate matter (PM). Therefore, the US

75 EPA's SPECIATE database is an important product to convert total emissions from specific sources

76 into the speciated emissions needed for the chemical transport model. The previous study has

77 combined the US EPA's SPECIATE database and air quality model to predict dust aerosols (Ying et

78 al., 2018), based on the assumption of the chemical composition of dust aerosols is similar to the

79 resuspended soil profiles.

80 Yet, dust generation and aerosolization are complex processes, which may have some chemical

81 selectivity. Most small dust particles (< 20 μm) are produced either by wind erosion, which leads to

82 soil movements such as creeping, saltation, and suspension (Burezq, 2020) or sandblasting process,

83 which leads soil particles (~75 μm) to be lifted by the wind, move in ballistic trajectories due to the

84 combined effect of aerodynamic force and gravity force (Grini and Zender, 2004; Shao and Raupach,

85 1993; Shao et al., 1996). The sandblasting efficiency of a soil particle is highly sensitive to its size

86 (Grini and Zender, 2004; Grini et al., 2002). In addition, the chemical composition of soil particles

87 can also vary with particle size. As smaller soil particles are more easily ejected, dust aerosol

88 particles are unlikely to have exactly the same composition as their parent soils (Perlwitz et al., 2015;

89 Wu et al., 2022). Dust deposited samples were the dust samples collected on the road or other

90 surfaces using a brush and plastic tray (Shangguan et al., 2022), while dust aerosol samples were

91 collected by filtering the air. Dust aerosols were produced by the ballistic impacts of wind-driven

92 sand grains (Kok et al., 2023). Indeed, some previous studies do find that in the deposited dust

93 samples (not dust aerosol samples), smaller particles tend to contain higher amounts of heavy metals

94   (Naderizadeh et al., 2016; Parajuli et al., 2016; Becagli et al., 2020). However, the heavy metal

95   profiles for dust aerosols from the US EPA's SPECIATE database seem to have no such enrichment

96   between each particle size, as Table S1 reports profile 41350 as an example. Although these profiles

97   have been widely used in air quality modeling works (Lowenthal et al., 2010; Simon et al., 2010;

98   Ashrafi et al., 2018), they were actually measured in the 1970s and 1980s with the resuspension of

99   soil samples, which placed soil in a glass tube and drew air flow to blow and suspend the soil

100   particles to the air (Miller et al., 1972). This method is not likely to produce realistic dust aerosols,

101   as it does not simulate sandblasting process properly. It is not known whether using such a

102   problematic dust profile could significantly impact air quality model calculations.

103

104   Here we examined the enrichment of heavy metals in the laboratory-generated dust aerosols. A dust

105   aerosol generator that mimics realistic sandblasting and saltation was used to generate dust aerosol

106   from a collection of soil samples (Lafon et al., 2014). The concentrations of heavy metals in soil

107   and dust aerosols were measured by an inductively coupled plasma mass spectrometer (ICP-MS).

108   In this study, some heavy metals, such as Mn, Cd, Zn and Pb, were found to be highly enriched in

109   dust aerosols. Especially, the enrichment factors would be much higher for smaller dust aerosols. In

110   addition, we also utilized a single particle aerosol mass spectrometer (SPAMS) to study heavy metal-

111   containing dust aerosols before, during, and after a dust storm. Regional air quality models usually

112   use problematic dust composition profiles from the US EPA's SPECIATE database. Herein we

113   modeled the contribution of dust aerosol to atmospheric heavy metal loadings, utilizing a range of

114   dust aerosol profiles determined in this laboratory study as well as the SPECIATE profile, to

115   investigate whether using a proper dust profile is critical to air quality modeling and cancer risk

116   calculations.

2 Materials and methods

2.1 Soil sample collection

119   Fourteen samples were collected from the top 10 cm of the natural soil profile from various locations

120   in dust source regions and Shanghai, China (Table S2, Fig. S1). S1-S4 were collected from dust

121   sources on the northern slope of Yinshan Mountain in central inner Mongolia and the adjacent areas

122   of the Hunshandake Sandy Land, S5-S12 were collected from dust sources of Hexi Corridor and

123   Alxa Plateau, S13 was collected in Xinjiang Province, in the dust sources of the Taklimakan Desert,

124   and S14 was sampled from Shanghai Yangpu District. Although the soil (S14) collected in Shanghai

125   does not originate from a dust source region, it can still produce dust aerosols in some cases. For

126   example, under dry weather conditions, the soil surface in the Shanghai area could serve as a

127   significant local contributor to the generation of dust aerosols (Liu et al., 2016; Liu et al., 2020).

128   During the prevailing dust storm periods from March to May, Shanghai is primarily influenced by

129   dust originating from the western Inner Mongolia Gobi, deserts in the Tibetan Plateau, and arid

130   deserts in northwest China (Fu et al., 2010; Fu et al., 2014; Sun et al., 2017). Soil texture

131   determination was conducted according to the method outlined in a previous study (Kettler et al.,

132   2001). Soil texture characterization was conducted based on the method outlined in a previous study

133   (Kettler et al., 2001). Soil particle dispersion was achieved by adding hexametaphosphate (HMP)

134   and sodium hydroxide (NaOH) to a soil sample (particle size< 2 mm) and shaking it for 16 hours.

135   The percentage of sand and silt was obtained using a Laser Scattering Particle Size Distribution

136   Analyzer (LA-960). Further details can be found in the SI. As shown in Table S2, they represent

several soil types: S1 was silty loam; S2, S4, S7, S10, S11 and S12 were sand; S3 was sandy loam; S5 and S6 were loam; S8 and S13 were loam sand; S9 and S14 were silty clay loam. Before dust aerosol generation, soil samples were placed in a fume hood and left to dry, without stirring or other treatment, before aerosolization. Fine and coarse dust aerosols ($PM_{2.5}$ and PM_{10}) were produced with a GAMEL dust aerosol generator, which can realistically simulate the sandblasting process. Then, the pH of the soil was measured. Detailed information can be found in Fig. S1 and Table S2.

2.2 Laboratory dust aerosol generation and collection

A laboratory dust generator (GAMEL: "Générateur d′Aérosol Minéral En Laboratoire") (Lafon et al., 2014) was used to produce dust aerosols from the soil samples. The GAMEL dust generator can realistically simulate the sandblasting process. Wind tunnels have the advantage of realistically simulating the generation of dust aerosols. However, conducting this study has certain drawbacks. These include the requirement for a substantial quantity of parent soils and the significant cost associated with eliminating ambient aerosol interference (Alfaro et al., 1997; Lafon et al., 2006; Alfaro, 2008). In GAMEL's dust production system, 10 g of each soil sample was added to a PTFE flask, which was agitated by a shaker simulating the sandblasting process to produce dust aerosols. A constant flow of particle-free air was passed through the dust-generating flask. The optimal generation parameter of the shaker was set at a frequency of 500 cycles/min according to Lafon et al., 2014 with an airflow rate of 8 liter/min controlled by a Mass Flow Controller (MFC, Sevenstar, Beijing Sevenstar Flow Co., LTD). The sample stream was filtered through a cyclone and particles were collected on a 47 mm PVC film held in a metal frame filter holder (Pall Gelman, Port Washington, NY, USA). Dust-$PM_{2.5}$ and dust-PM_{10} were obtained with or without an 8LPM cyclone,

158 respectively. The running time was 1min. To obtain more dust aerosols in different size ranges, size-

159 fractionated particle sampling of dust aerosols was carried out with a 10-stage Micro-Orifice

160 Uniform Deposit Impactor (MOUDI 110R; MSP) with size cut points of 10 μm, 5.6 μm, 3.2 μm,

161 1.8 μm, 1.0 μm, and 0.56 μm. Analysis of the size distribution and chemical composition of dust

162 generated by GAMEL and dust generated under natural conditions has shown that the GAMEL

163 generator can produce realistic dust aerosol (Lafon et al., 2014). All the dust aerosol mass collected

164 is shown in Table S3 and S4. The instrument setup is illustrated in Fig. S2.

165

166 **2.3 Analysis of laboratory-generated dust aerosols**

167 The dust aerosol samples collected were weighed with an analytical balance and then put into 25 ml

168 digestion tubes with 6 ml 69% HNO_3 symmetrically. The temperature program of Microwave

169 Digestion (Anton Paar) was as follows: initial temperature of 100 °C held for 5 min, then ramped

170 to 140 °C for 5 min, and finally at 180 °C for 60 min. The whole process was holding 120 min.

171 According to this study (Chang et al., 1984), almost all the heavy metal elements in the natural soil

172 and dust aerosol in concentrated nitric acid were extracted using this experimental procedure. After

173 digestion, the solution was acid-fed at 120 °C for 1.5 h, then deionized water (conductivity 18.25

174 MΩ) was added, the volume was constant with a 25 mL volumetric flask and then passed through a

175 0.45 μm membrane. The samples were diluted with 2% HNO_3 by 4 times for further analysis. Three

176 blank PVC film samples were digested using the same method for background control.

177

178 The heavy metal content was determined by an inductively coupled plasma mass spectrometer (ICP-

MS; Agilent, 8900). Before analysis, tuning procedures including plasma parameter, ion transmission path, quadrupole mass spectrometer, and detector had been done. During analysis, standard solutions were prepared at concentrations of 0, 1, 2, 5, 10, 20, 50, and 100 μg/L. "In, Bi, and Rn" were used as internal standard elements, and were introduced into the nebulizer by mixing with the sample to be tested and the standard solution in the sampling pipeline by online addition, and the instrument drift and matrix effect were compensated. After each analysis of a sample, 2% dilute nitric acid was used to clean the injection line for 1 min, and then continue to collect the second sample to eliminate the memory effect of the previous sample.

A scanning electron microscope (SEM; Phenom Pro) equipped with an energy-dispersive X-ray detector was used for morphologies of particle examination at the voltage of 10 kV. All the samples (soil, $PM_{2.5}$ and PM_{10}) were on the carbon conductive adhesive, then spray platinum to improve the conductivity. Here, the parent soil of S10 and generated $PM_{2.5}$ and PM_{10} were examined.

Statistical analysis was performed using SPSS Statistics. The correlation analysis was conducted through Spearman's correlation and the significant difference was used with an independent sample T-test.

2.4 Ambient dust aerosol measurements

On May 23rd, 2018 (LT), on-site field measurements were conducted in Shanghai to assess the ambient dust particles. The measurements indicated an average wind speed of 2.2 m/s, which corresponds to a level of a floating dust storm with a visibility of up to 10 km. The sampling was located on the sixth floor of the Environmental Science Building in Jiangwan Campus, Fudan University, a typical residential area in a heavily polluted urban area. The chemical composition of

individual ambient particles was measured by single-particle aerosol mass spectrometry (SPAMS, Hexin Co., Ltd). Detailed information on SPAMS is available elsewhere (Li et al., 2011). An adaptive resonance theory-based clustering method (ART-2a) was used to classify the mass spectra generated and identify dust/heavy-metal-containing particles (Sullivan et al., 2007). The Hybrid Single-Particle Lagrangian Integrated Trajectory HYSPLIT-4 model developed by the ARL (Air Resources Laboratory) of the NOAA (National Oceanic and Atmospheric Administration), USA, was employed to compute hourly resolved 48 h air mass backward trajectories at 500 m arrival height (Lv et al., 2021; Pongkiatkul and Kim Oanh, 2007).

2.5 Air quality model configuration and application

The source-oriented Community Multiscale Air Quality (CMAQ) model v5.0.1 with an expanded Stratospheric and Air Pollution Research-99 (SAPRC-99) photochemical mechanism was applied to simulate $PM_{2.5}$ levels and track the sources of primary $PM_{2.5}$ ($PPM_{2.5}$) in China during the entire year of 2013 (Guenther et al., 2012; Ying et al., 2018). The simulation domain covered China and its surrounding countries, with a horizontal resolution of 36×36 km^2 (127×197 grids). Anthropogenic emissions were based on the Multi-resolution Emission Inventory for China (MEIC, v1.3, $0.25° \times 0.25°$, http://www.meicmodel.org). Biogenic emissions were generated by the Model of Emissions of Gases and Aerosols from Nature (MEGAN) v2.1 (Guenther et al., 2012). The meteorological inputs for the CMAQ model were calculated by the Weather Research and Forecasting (WRF) model (https://www2.mmm.ucar.edu/wrf/users).

221   Five major source contributions (windblown dust, residential, transportation, power generation and

222   industrial sources) to PM$_{2.5}$ were investigated based on the inventory-observation-constrained

223   emission factors (Ying et al., 2018). Three control trials were conducted for each heavy metal

224   according to measured soil, dust-PM$_{2.5}$ and the SPECIATE datasets from the four regions (three dust

225   sources and Shanghai). It is worth noting that the emission factors for areas outside these four

226   regions were estimated using Inverse Distance Weight (IDW) spatial interpolation methods. These

227   methods were based on the dataset of emission factors within these four regions, which represent

228   the amount of heavy metal emitted per kilogram of dust (Zhang and Tripathi, 2018). Each heavy

229   metal source concentration from dust aerosol and all four sources were used to quantify the

230   contribution on heavy metal concentrations in the atmospheric dust aerosols, which can be

231   represented in Equation 1:

232
$$R = \frac{E_1 \times s_1 \times a}{\sum_{i=1}^{5} E_i \times s_i} \qquad\qquad \text{Equation 1}$$

233   Where E_i is the PPM$_{2.5}$ emission from i^{th} source, s_i is the emission factor of the specific heavy metal

234   from i^{th} source, a is a is the concentration of heavy metal in measured soil, dust-PM$_{2.5}$, and the

235   SPECIATE datasets. E_1, s_1, and a are the values for dust.

236   In addition, the human health risk of heavy metals was assessed. Three main routes of chemical

237   daily intake (CDI, mg kg^{-1} day^{-1}) of air heavy metals were: (1) direct ingestion of particles or gases

238   existed in the air (CDIing); (2) inhalation of suspended particles through mouth and nose (CDIinh);

239   and (3) daily absorption of heavy metals through the skin (CDIdermal) (Luo et al., 2012). To assess

240   the carcinogenic and non-carcinogenic effects of heavy metals, we evaluated these effects in 13 age

241   groups ranging from birth to ≤80 years old. These age groups are as follows: <1, 1 to <2, 2 to <3, 3

242   to <6, 6 to <11, 11 to <16, 16 to <20, 21 to <31, 31 to <51, 51 to <61, 61 to <71, 71 to <81, and ≥81

243   years (Gholizadeh et al., 2019b). The variables and values used for estimating human exposure to

244   heavy metals were obtained from the U.S. Environmental Protection Agency (USEPA) and the U.S.

245   Department of Energy (USDoE) (Moya et al., 2011; Doe, 2011). CDIing, CDIinh, and CDIdermal

246   were calculated as:

247

248 $$CDI_{ing} = C \times \frac{IRing \times EF \times ED}{BW \times AT} \times 10^{-6} \qquad \text{Equation 2}$$

249 $$CDI_{dermal} = C \times \frac{SA \times AF \times ABS_d \times EF \times ED}{BW \times AT} \times 10^{-6} \qquad \text{Equation 3}$$

250 $$CDI_{inh} = C \times \frac{IRinh \times ET \times EF \times ED}{BW \times AT} \times 10^{-6} \qquad \text{Equation 4}$$

251 Moreover, the total carcinogenic risk

252 (TCR) for each heavy metal were calculated by:

253 $$carcinogenic\ risk = CDI_{ing,dermal,inh} \times CSF \qquad \text{Equation 5}$$

254 $$TCR = \sum risk = CDI_{ing} \times CSF_{ing} + CDI_{inh} \times IUR +$$

255 $$CDI_{dermal} \times CSF_{ing}/ABS_{GI} \qquad \text{Equation 6}$$

256

257   Here the IRing was Ingestion rate (mg day^{-1}), EF was exposure frequency (day year^{-1}), ED was

258   exposure duration (year), BW was body weight (kg), AT was Averaging time (day), SA was total

259   body skin surface area (m^2), AF was skin adherence factor (mg cm^{-2}), ET was exposure time (hour

260   day^{-1}), ABSd was dermal absorption factor, IRinh inhalation rate (m^3 day^{-1}), ABS$_{GI}$ was

261   gastrointestinal absorption factor, CSF was cancer slope factor. The values of these parameters could

262   be found in the previous study (Gholizadeh et al., 2019a).

263

3 Results and discussion

3.1 Enrichment of heavy metals in fine dust aerosols

Fig. S3-S4 show the absolute concentrations of heavy metals in dust aerosols and their parent soils. The concentrations of heavy metals in dust-PM_{10} were similar to soil concentrations, which showed a significant correlation between soils and PM_{10} ($p<0.01$) (Fig. S5). While the concentrations of heavy metals in dust-$PM_{2.5}$ were higher than those in soils, especially Mn, Ni, Cu and Zn, showed significant differences ($p<0.001$) (Fig. S6). This trend was consistent across all soil samples. The enrichment factor (EF) of heavy metals in dust aerosols relative to the parent soils was calculated with Equation 7.

$$EF = \frac{C_1/m_1}{C_0/m_0} \qquad \text{Equation 7}$$

Where C_1 is the heavy metal concentration in dust-PM; m_1 is the mass of dust-PM collected on the filter; m_0 is the mass of soil in the ICP-MS sample, and C_0 is the heavy metal concentration of the soil.

Figures 1 and S7 show that many heavy metals were highly enriched in fine dust aerosols ($PM_{2.5}$), i.e., their absolute concentrations were significantly higher in fine dust particles than in the parent soil (Fig. S6). V, Cr, Mn, Co, Ni, Cu, Zn, As, Cd, Ba, Ti, and Pb were all enriched in dust-$PM_{2.5}$ during the process of dust formation. The following trend of heavy metal enrichment was established for dust-$PM_{2.5}$: Cd > Zn > Ba > Cu > Mn > Pb > Ni > Ti > Co > As > Cr > V. Notably, the EFs of Cd were greater than 5 for soil S1, S10 and S11. No other literature has reported the enrichment of Cd or other heavy metals in dust aerosols. However, there is one study showing the

enrichment of water-soluble ions during dust aerosol production from soil (Wu et al., 2022). It

reports that the EFs of Ca^{2+} ranged from approximately 5.6 to 223.1, and the EF values of Mg^{2+}

were between approximately 2.1 and 90.3 for dust-$PM_{2.5}$ from Sandy soils in the Taklamakan Desert.

In this study, it is found that the EF of Cd and other metals falls within the range of EF for these

water-soluble ions, consistent with the value reported by Wu et al., (2022). Fig. 1 also illustrates

that all heavy metals were more highly enriched in smaller $PM_{2.5}$ dust particles compared to larger

PM_{10} dust particles. For example, the Cd's EF reached ~6.4 and ~1.7 for dust-$PM_{2.5}$ and dust PM_{10},

respectively, from soil S1. Most dust-$PM_{2.5}$ should originate from the small colloids in soil, which

are defined as soil particles with less than 2 μm in diameter. These soil colloids usually carry large

amounts of negative charges, which can help adsorb many cations in soil, including various heavy

metal ions (Brady and Weil, 2008). Thus, heavy metals are enriched in small soil aggregates. During

the sandblasting process, the smaller soil grains, with higher heavy metal concentrations, are more

likely to be ejected and form dust aerosols. The particle size dependence of heavy metal enrichment

could have significant ramifications for the health impacts of dust aerosols. The dust aerosol size

distribution of dust (Fig. S8) was also measured by an Aerodynamic Particle Sizer (APS,

APS Model 3321; TSI Inc.; USA). It is found that the peak of the particle size distribution of dust

aerosol was approximately at 2~3 μm. Similarly, the scanning electron microscope (SEM) images

of these dust aerosols (generated by S10) also show the presence of a large number of particles with

sizes of 2~3 μm. As particle size decreased, the shape of particles changed from flakes to rods,

which means a larger surface area (Fig. S9). When examining the impact of soil texture on dust

aerosol enrichment, first, notable variations were observed in the EF values from one soil texture,

such as sandy soils, specifically S2, S4, S7, S10, S11, and S12. To assess the significance of these

308   variations, a one-way Analysis of Variance (ANOVA) was conducted using SPSS. In ANOVA, the

309   *p-value* represents the probability of obtaining the observed differences in means (or more extreme

310   differences) by random chance alone, assuming no true difference between the groups. A *p-value*

311   below a predetermined significance level (commonly 0.05) indicates significant differences between

312   the means of the compared groups. Specifically, for sandy soil, analysis results reveal significant

313   variations between these six soils in terms of the EF values for both dust-$PM_{2.5}$ (*p-value*=0.004<0.05)

314   and dust-PM_{10} (*p-value*=0<0.05) (Table S5 and S6). These results indicate that there are significant

315   differences in the EFs of heavy metals within the sandy soil group. Then, the variation between soil

316   types was analyzed. For the six different types of soil samples, the results of ANOVA showed

317   significant differences in the EFs of dust-$PM_{2.5}$ (*p-value* =0<0.05) and dust-PM_{10} (*p-value* =0<0.05)

318   among these soil types (Table S7 and S8). The differences among the six soils from different soil

319   types were greater than those observed among the different soils in the same soil type, indicating a

320   potential role of soil type in affecting EFs, which would require further study to elucidate. Detailed

321   information was found in SI of Texture S3 and Table S5-S10.
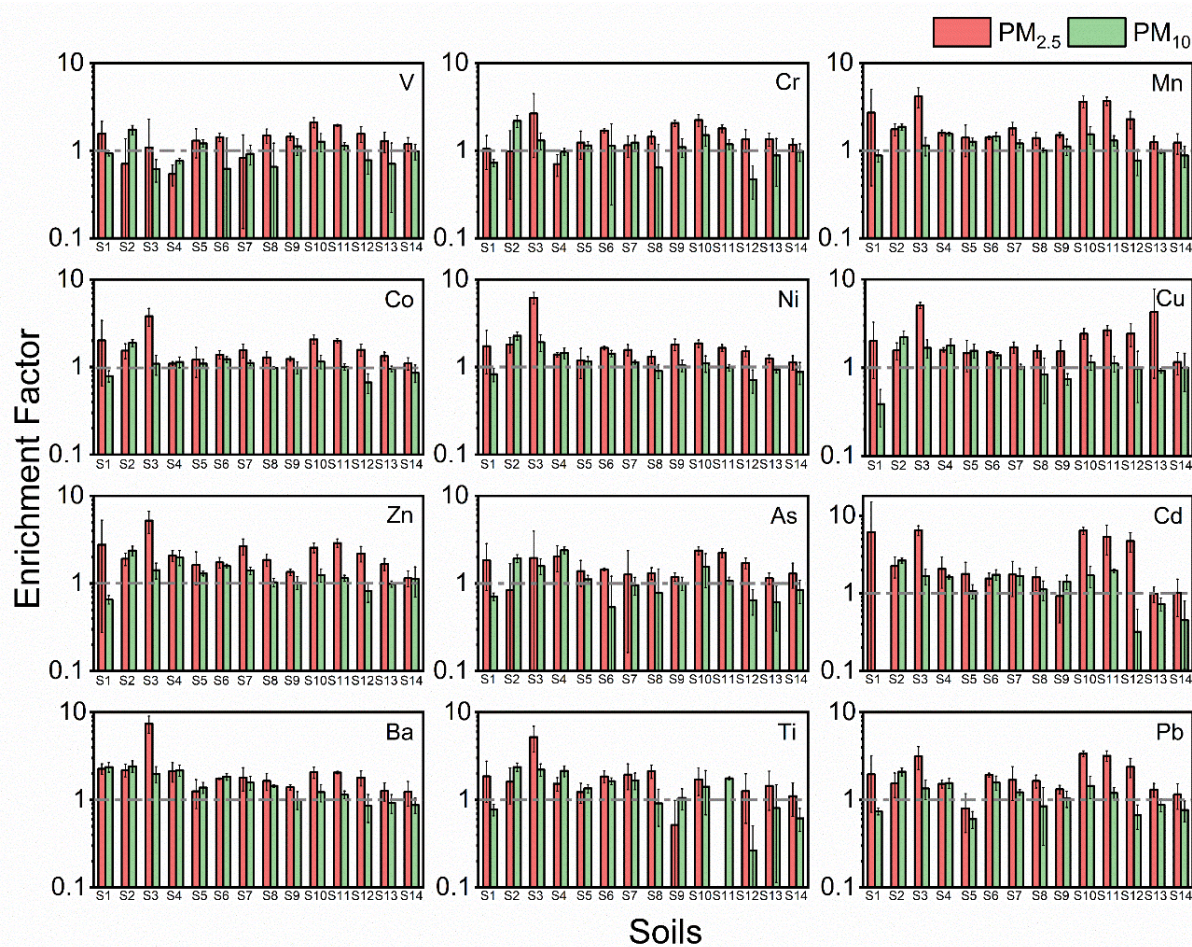
Figure 1. Enrichment Factors of $PM_{2.5}$ and PM_{10}. Enrichment factors of heavy metals in dust aerosols from soil S1-S14; red represents $PM_{2.5}$ and green represents PM_{10}. The grey dotted line represents the EF as 1. The whiskers on the bars represent the standard deviations of triplicates.

To investigate the link between dust particle size and heavy metal EFs in greater detail, a MOUDI impactor was used to collect dust-PM from 0.56 to 10 μm (absolute concentration obtained in Fig. S10). Consistent with the results discussed above, the EFs for some heavy metals, such as Pb, significantly increased with decreasing particle diameter (r= -1, p < 0.01) (Fig. 2). For the smallest dust particles (0.56~1.0 μm), the EFs for Pb was approximately 83, an order of magnitude greater than the EFs (~3) for the largest dust particles (>10 μm). V, Cr, Co, Mn, Ni, Cu, Zn, As, and Ba show consistent trends, with EFs increasing as the particle size decreases. In detail, V (ranging from

334 ~1.1 to ~18.9), Cr (ranging from ~1.5 to ~23.7), Co (ranging from ~1.7 to ~93.7), Mn (ranging from

335 ~2.3 to ~7.4), Ni (ranging from ~1.6 to ~29.7), Cu (ranging from ~3.3 to ~54.3), Zn (ranging from

336 ~2.3 to ~19.0), As (ranging from ~1.8 to ~112.3), and Ba (ranging from ~1.4 to ~7.0), as the particle

337 size decreases from 10 μm to 0.56 μm. These results demonstrate that some heavy metals are indeed

338 enriched in smaller soil particles, which could be aerosolized during the sandblasting process. The

339 particle size dependence of heavy metal enrichment could have significant ramifications for the

340 health impacts of dust aerosols. In contrast, Cd's EFs remain relatively unchanged with varying

341 particle sizes. On the other hand, Ti exhibits an opposite trend, with EF values decreasing as the

342 particle size decreasing, and the reason for this difference requires further study.
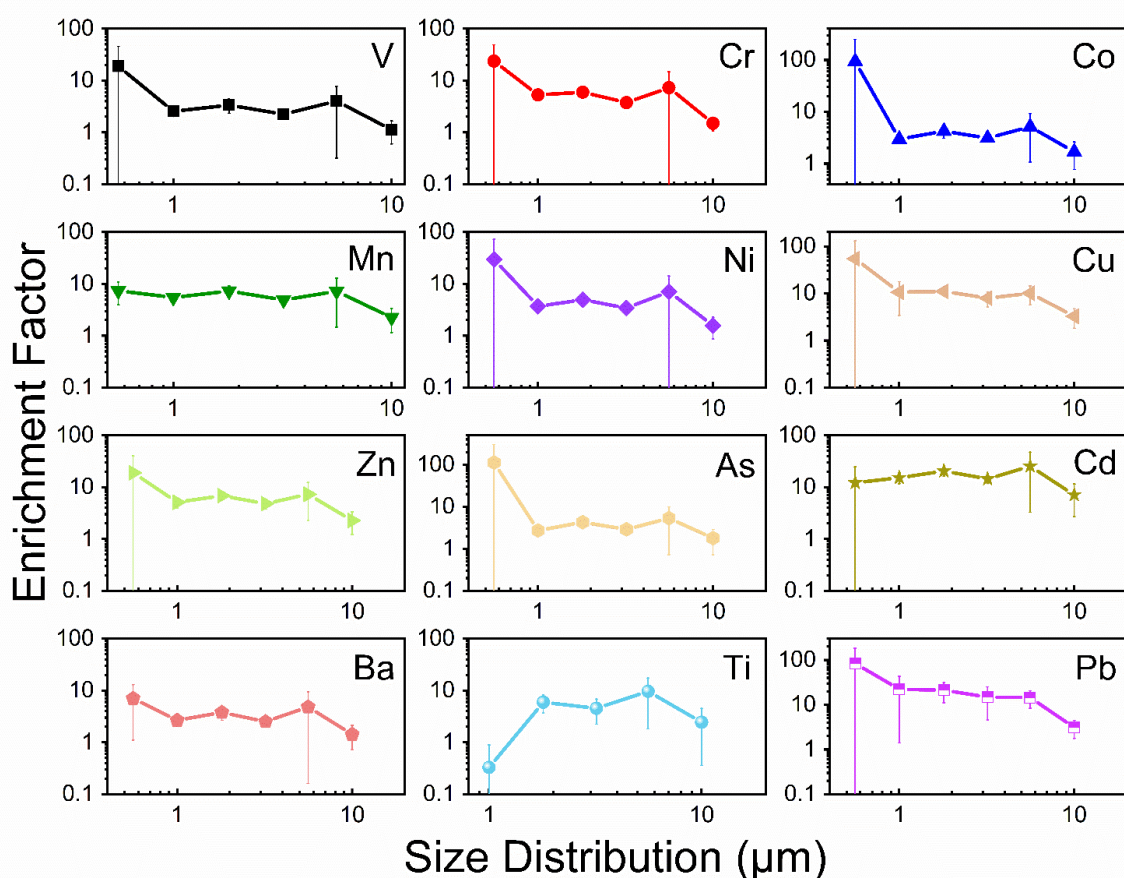
343

344 **Figure 2.** Enrichment factors of heavy metals in dust aerosols with different particle size ranges.

345 The EF data were produced from the Soil S10, with diameters at above10 μm, 5.6-10 μm, 3.2-5.6

346 μm, 1.8-3.2 μm, 1.0-1.8 μm and 0.56-1.0 μm. The whiskers on the bars represent the standard

347 deviations of triplicates.

348

3.2 Modeling of the contributions of dust aerosols to atmospheric heavy metals using the dust profiles from this study and the SPECIATE datasets

351 It is necessary to know the sources of atmospheric heavy metals to effectively control their emission.

352 Air quality models with emission inventories can estimate the contributions of various sources to

353 atmospheric heavy metals. However, when estimating heavy metal emissions from dust production,

354 some widely used air quality models, such as the CMAQ model, typically use dust profiles from the

355 US EPA's SPECIATE datasets. As discussed in the introduction, this dust profile may be outdated

356 and cannot reflect realistic dust compositions. We used the CMAQ model to assess the potential

357 impact of dust aerosol profile in atmospheric dust aerosol using our measured profile and the profile

358 (No. 41350) from the SPECIATE datasets. The model tracked heavy metals in $PM_{2.5}$ in China for

359 the year 2013 (see Methods) from five major sources: windblown dust, residential, transportation,

360 power generation, and industry.

361

362 Figure 3 shows the modeled contributions of the dust source to the Cr and Pb concentrations in

363 $PM_{2.5}$ for China, using the measured soil, dust-$PM_{2.5}$ profiles from this study, as well as the

364 SPECIATE composition profiles (see Methods). In addition, the modeled results for other metals,

365 such as As, Cu, Mn, Ti, and Zn were presented in Fig. S11-15.

366

367 For atmospheric Cr, it is clear that the scenario of applying SPECIATE database significantly

368 underestimates the contribution of dust aerosol, with the highest value of ~0.08 $\mu g/m^3$, when

369   compared to the scenario of applying the measured dust-PM$_{2.5}$ profiles, which had the highest value

370   of ~0.14 $\mu g/m^3$. For Pb, as shown in the right column of Fig. 3, the scenario of applying

371   SPECIATE profile overestimates the contribution of dust aerosol, with the value up to ~0.4 $\mu g/m^3$,

372   when compared to the scenario of applying the measured dust-PM$_{2.5}$ profiles, which had the highest

373   value of ~0.14. Uncertainties associated with the use of SPECIATE have also been identified in

374   previous studies (Ho et al., 2003; Xia et al., 2017). Specifically, the dust PM$_{2.5}$ source profiles

375   obtained from local studies indicated that SPECIATE overestimated the contributions of

376   atmospheric K and Al by approximately 23%, while underestimating the contributions of Ca and

377   Na by 50%. Additionally, the model represents the annual average data for the year 2013. Although

378   there are some field studies conducted in the same year (Wang et al., 2021; Shi et al., 2018), there

379   is no available annual average data for a direct comparison with the model results. These results

380   demonstrate that the modeled heavy metal distribution in the atmosphere is quite sensitive to the

381   input of dust composition profile, strongly suggesting that using a proper dust composition profile

382   is a key in such air quality modeling.

383

384   As discussed in the Introduction, many atmospheric studies assume that dust aerosol composition

385   is similar to the composition of its parent soil. Here we also use the soil composition as an input

386   dust profile in the model calculation to see how the modeled results are compared to that using the

387   dust-PM$_{2.5}$ profile. For Cr, an obvious elevation of contribution was found by comparing the map

388   using soil (a) and dust-PM$_{2.5}$ (b) profiles, with the hotspots of contribution (~0.14 $\mu g/m^3$)

389   distributed in northwest China. The region with dust aerosol contribution ranged from 0.02 to 0.08

390      $\mu g/m^3$ covers most areas in China by using the dust-PM$_{2.5}$ profile. In contrast, the application of

391   the soil profile to the model reveals a significantly reduced area where the modeled Cr concentration

392   from dust aerosols falls within the range of 0.02 to 0.08 $\mu g/m^3$. For Pb, a significant difference is

393   also found. The high contribution areas are also mainly distributed in northwest China for scenarios

394   of applying soil and dust profiles, with a value up to 0.1 $\mu g/m^3$. While the area with low dust

395   aerosol contribution (<0.02 $\mu g/m^3$) shrinks considerably in the scenario of applying soil profile.

396

397   The applied dust enrichment factors to modeled Cr in PM$_{2.5}$ had an even stronger impact on modeled

398   source apportionment (Fig. 3a-3b). The average dust source contribution to the total PM$_{2.5}$ Cr

399   concentration over China was calculated to be 0.03, and 0.05 $\mu g/m^3$ in the scenarios of applying

400   soil and dust profiles, respectively. The model results for As, Cu, Mn, Ti and Zn (Fig. S11-S15) also

401   show similar trends, indicating applying realistic enrichment factors to heavy metal concentrations

402   in fine dust aerosols is critical to accurately model the sources of atmospheric heavy metals. These

403   results demonstrate that it is not appropriate to assume dust aerosol composition is equal to soil

404   composition, at least in air quality modeling.
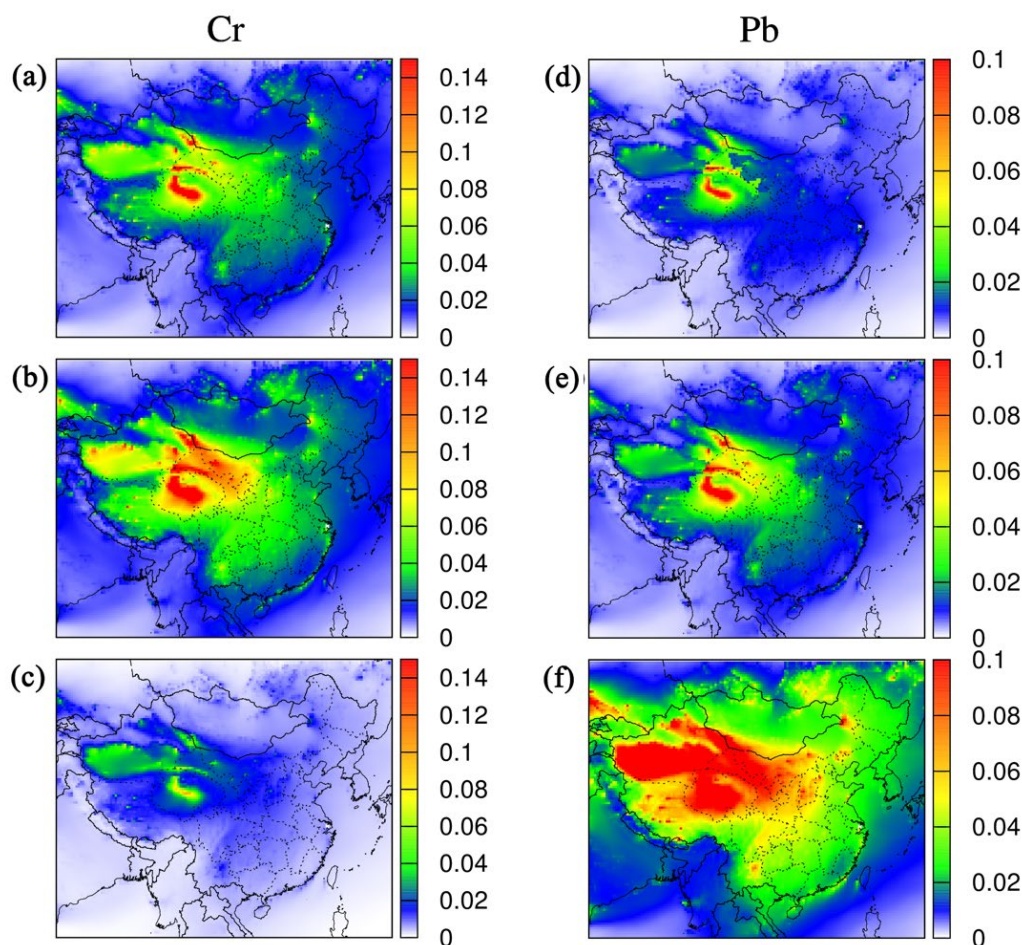
Figure 3. Modeling of the contributions of dust aerosols to atmospheric Cr and Pb concentrations. These results use the dust profiles of measured soil (a, d), dust-PM$_{2.5}$ (b, e), and the SPECIATE datasets (c, f). The unit is $\mu g/m^3$.

Figure 4 shows the Total Carcinogenic Risk (TCR) of the modeled atmospheric heavy metals (Cu, Pb and Zn) for each province in Mainland, China. The modeled results using the dust-PM$_{2.5}$ and the SPECIATE profiles are compared here. The carcinogenic risks lower than 10^{-6} are considered negligible, and risks above 10^{-4} are not accepted by most international regulatory agencies (Cheng et al., 2015; Epa, 1989; Luo et al., 2012). For Cu, it is evident that using the SPECIATE profile overestimated (the difference ranges up to $\sim 7.5 \times 10^{-7}$) the TCR in China compared to using the dust-PM$_{2.5}$ profile, as some regions exceed 10^{-6}, the threshold value. For Pb, although all regions were above 10^{-6}, the TCR using the SPECIATE profile was greatly overestimated (the difference range is

417   ~ 5.5×10^{-6} - 4.0×10^{-5}). The model results for Zn showed that all regions were not above 10^{-6} but

418   significantly underestimated risks using the SPECIATE profile. This indicates that the health risk

419   assessment is also sensitive to dust composition profiles. Using the SPECIATE profile might be

420   problematic for assessing these risks.
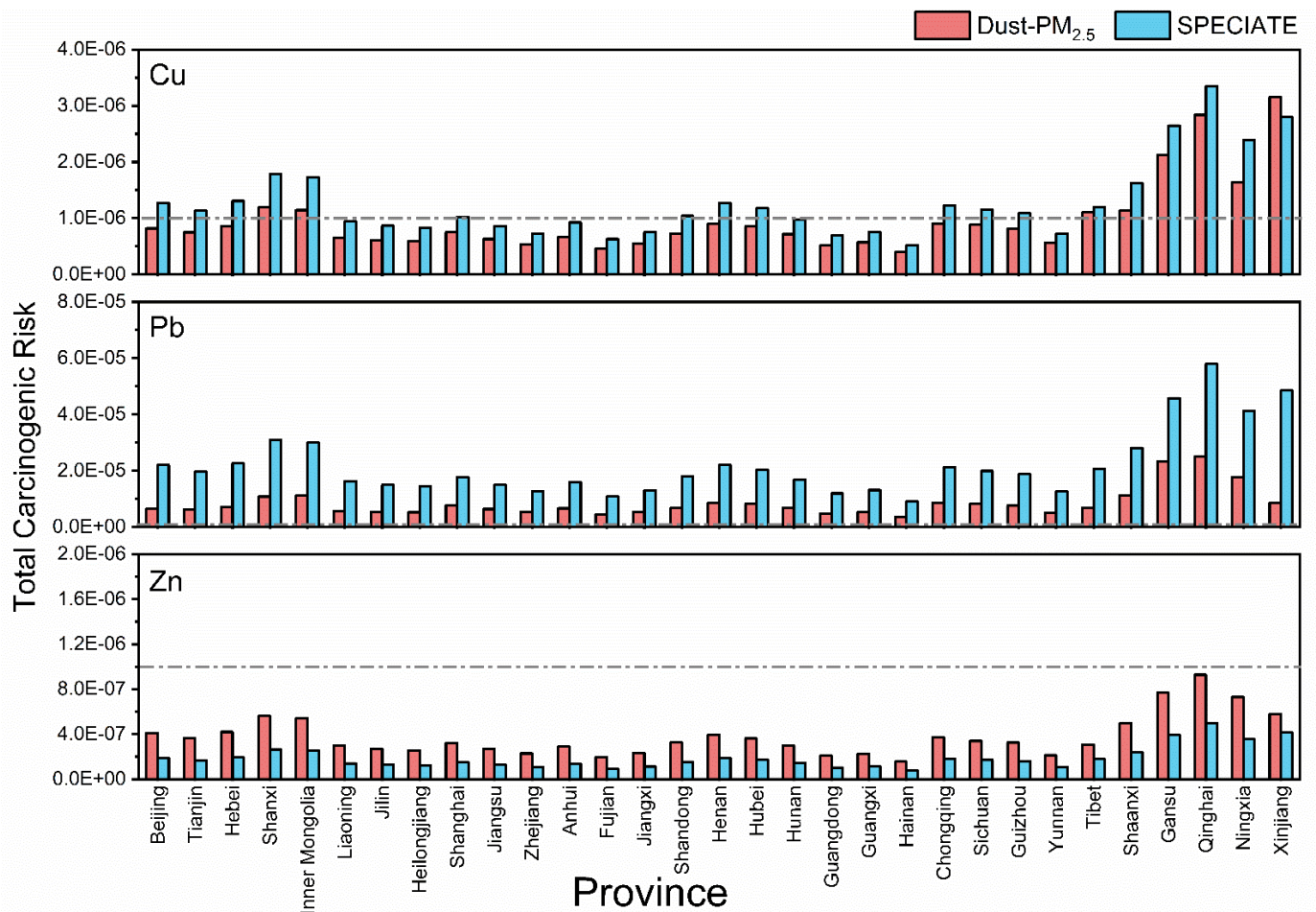
421

422   **Figure 4.** Comparison of the total carcinogenic risk (TCR) of the modeled atmospheric heavy metals

423   for each province in Mainland, China between using the dust-$PM_{2.5}$ and SPECIATE profiles. Here,

424   the TCR of Cu, Pb and Zn were calculated. The grey dotted line is 10^{-6}, the threshold value for

425   health concerns.

426

3.3 Field observation before, during and after a dust storm

Our modeling results suggest that dust aerosol could be a major source of multiple heavy metals in $PM_{2.5}$ in China. Therefore, dust storms should significantly increase the concentrations of heavy metals in $PM_{2.5}$. To test this idea, we studied a dust-storm plume, which originated from Mongolia and arrived in Shanghai (Huang et al., 2010) on 23 May 2018 (Fig. S16). Real-time single-particle mass spectra were generated by a single-particle mass spectrometer. Single-particle mass spectrometry can offer detailed information on the chemically-resolved mixing state at the single-particle level. According to the similarities of the mass-to-charge ratio and peak intensity of characterized signals, *"Dust"* particles were classified via an adaptive resonance theory-based clustering method (ART-2a, see Method). The number fraction of *Dust* particles was ~4.94% before and after the dust storm and it increased to ~9.73% during the dust storm episode (Fig. 5a).

Dust particle mass spectra also contained ion markers indicative of an array of heavy metals (*m/z* 55[Mn^+], 51[V^+], 207[Pb^+], 63[Cu^+], 75[As^+], 91[AsO^+], 52[Cr^+], -84[CrO_2^-], -100[CrO_3^-]) (red sticks in Fig. S17), indicating the existence of heavy metals in the ambient dust aerosols. The time series of Pb-containing and Cr-containing particle number fractions showed similar trends to the *Dust* particles. When the dust storm arrived, both Pb-containing and Cr-containing particle fractions increased as the dust cluster fraction increased. Before and after the dust storm, the percentages of Pb-containing and Cr-containing particles that overlapped with the *Dust* cluster were 41% and 32%, respectively. However, this overlapped ratio increased to 86% and 71% during the dust storm episode. The increase of heavy metal particles in step with the dust particles indicated that the dust particles could be the dominant source of these heavy metal species during this dust storm episode.

449

450   We further analyzed the size-resolved number fraction of dust aerosol, Pb-containing, and Cr-

451   containing particles during the dust storm episode (Fig. 5b). The number fraction of *Dust* particles

452   increased with increasing aerodynamic diameter. For particles above 1.0 μm, *Dust* accounted

453   for >12% of the total particles during the storm. However, the Pb-containing and Cr-containing

454   particles made up a larger number fraction of analyzed particles with decreasing particle diameter

455   size (< 1 μm). The number fractions of Pb-containing and Cr-containing particles were 5.7% and

456   7.9% of all mass spectra for particles from 0.2-0.3 μm. This result was consistent with our laboratory

457   results that there is high heavy metal enrichment in smaller dust particles and our modeling results

458   that dust aerosol is likely a major source of atmospheric Pb and Cr over China.
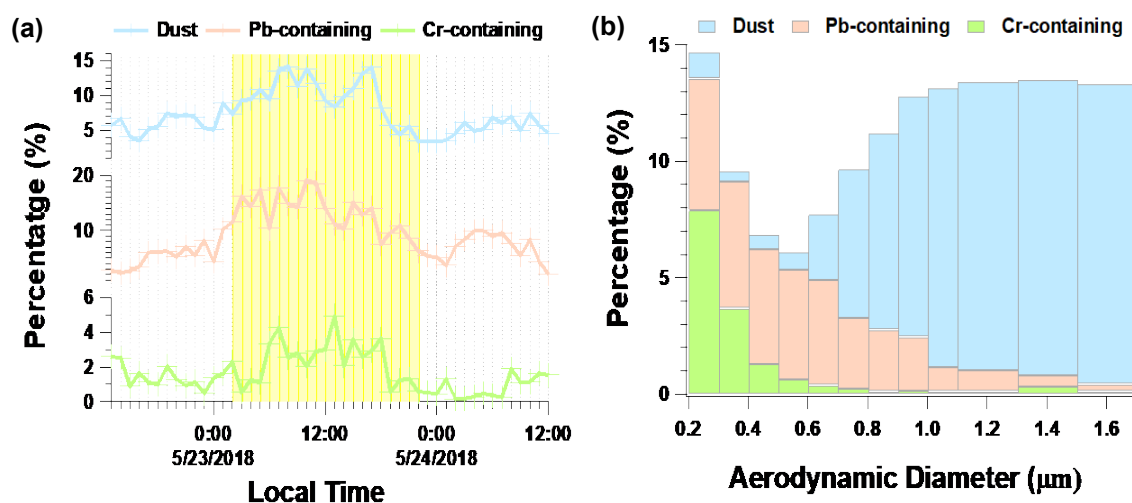
459

460   **Figure 5.** Ambient dust aerosol measurements. (a) Temporal variation of the percentages of dust

461   aerosol, Pb-containing, and Cr-containing particle clusters. The yellow shadow represents the dust

462   storm episode. (b) Size-resolved number fraction of dust aerosol, Pb-containing, and Cr-containing

463   particle clusters.

464

4 Environmental implications

In this study, many heavy metals were found to be highly enriched in fine (PM$_{2.5}$) dust aerosols compared to their concentrations in the parent soils. We propose that heavy metals tend to be enriched in smaller soil aggregates (Ikegami et al., 2014). During the sandblasting process, the heavy metal enriched smaller soil aggregates are more likely to be ejected and form dust aerosols. This work finds that dust aerosols from different soils may have a range of heavy metal enrichment factors. To study the transfer of heavy metals from soils to the air, it is critical to have a complete set of enrichment factors for each major soil type. There exists a difference among the heavy metal enrichment factors from different soil samples. The variability in the EFs is likely due to differences in soil properties (soil texture and size distribution etc.) which may affect the sandblasting/saltation process. For example, the enrichment factors of heaviest metals for Soil S1, S10 and S11 were higher than other soils. The detailed reason is still unknown and needs further exploration. Moreover, air quality models, including CMAQ models and various CMB models, often use the dust chemical profiles from the US EPA's SPECIATE to calculate the contribution of fine dust aerosols to atmospheric heavy metals, which are outdated and could lead to significant errors in estimating the emission of heavy metals through dust generation. Without using proper dust profiles in estimating heavy metal emissions from dust generation, the contribution of fine dust aerosols to atmospheric heavy metals, and its associated health risks are likely significantly mistaken.

5.Conclusions

Dust generation and aerosolization are complex processes that may have certain chemical selectivity.

485 Here, we deployed a laboratory generator to produce dust aerosol with a realistic sandblasting

486 process. The concentrations of heavy metals (including V, Cr, Mn, Co, Ni, Cu, Zn, As, Cd, Ba, Ti,

487 and Pb) in soils and fine ($PM_{2.5}$) and coarse (PM_{10}) dust aerosols were measured. With research

488 efforts to elucidate the enrichment process of heavy metal in dust aerosols compared to their parent

489 soils, our results fill the knowledge gaps of the compositional variation of heavy metal between the

490 parent soils and the generated dust aerosols. Mn, Cd, Pb and other heavy metals were found to be

491 highly enriched in fine ($PM_{2.5}$) dust aerosols, which can be up to ~6.5-fold. These findings were

492 also consistent with our field observation results. In addition, air quality models often use an

493 outdated heavy metal profile for dust aerosols from the US EPA's SPECIATE database, which seems

494 to lack enrichment between each particle size. We modeled the impact of the contribution of heavy

495 metals in dust aerosol and their health risks in CMAQ, a widely used air quality model, and

496 determined that atmospheric heavy metal concentrations over China, which drastically changed

497 when we applied different dust profiles, such as the measured soil, dust-$PM_{2.5}$ profiles from this

498 study, as well as the SPECIATE composition profiles. Our air quality modeling for China

499 demonstrates that the calculated contribution of fine dust aerosols to atmospheric heavy metals, as

500 well as their cancer risks, could have significant errors without using proper dust profiles.

Supplement

502 The supplement related to this article is available online at: http://dx.doi.org/ 0.17632/byg6xk2fg9.1.

Data availability

504 All data supporting this study and its findings will be available in an online data repository at:

http://dx.doi.org/10.17632/wpphf8rd33.1.

Author contributions

X.W. and J.C. conceptualized the work and designed the experiments. H.Z. and S.Z. led the air quality modeling work. Q.G. lead the experimental work of heavy metal enrichment measurements. J.Z. led the field observation. K.Z., Q.W., S.C., S.W., J.H., X.L. and H.C. helped in experimental works. L.Z., L.W., Z.W., X.Y. and H.Z. helped in the experimental design and data analysis. Q.Y. provided the data required for the air quality modeling. All authors contributed to the paper's writing.

Competing interests

The authors declare no competing interests.

Disclaimer

Publisher's note: Copernicus Publications remains neutral with regard to jurisdictional claims in published maps and institutional affiliations.

Acknowledgements

The authors also thank Xiangcheng Zeng for their help in heavy metal measurement.

Financial support

This work was partially supported by the National Natural Science Foundation of China (Nos. 92044301, 42077193, 21906024). Comments from Dr. Camille Sultana greatly improved this manuscript.

Reference

Alfaro, S. C.: Influence of soil texture on the binding energies of fine mineral dust particles potentially released by wind erosion, Geomorphology, 93, 157-167, 10.1016/j.geomorph.2007.02.012, 2008.

Alfaro, S. C., Gaudichet, A., Gomes, L., and Maille, M.: Modeling the size distribution of a soil aerosol produced by sandblasting, Journal of Geophysical Research-Atmospheres, 102, 11239-11249, 10.1029/97jd00403, 1997.

Ashrafi, K., Fallah, R., Hadei, M., Yarahmadi, M., and Shahsavani, A.: Source apportionment of total suspended particles (TSP) by positive matrix factorization (PMF) and chemical mass balance (CMB) modeling in Ahvaz, Iran, Archives of environmental contamination and toxicology, 75, 278-294, 2018.

Balakrishna, G. and Pervez, S.: Source apportionment of atmospheric dust fallout in an urban-industrial environment in India, Aerosol and Air Quality Research, 9, 359-367, 2009.

Becagli, S., Caiazzo, L., Di Iorio, T., di Sarra, A., Meloni, D., Muscari, G., Pace, G., Severi, M., and Traversi, R.: New insights on metals in the Arctic aerosol in a climate changing world, Science of The Total Environment, 741, 140511, https://doi.org/10.1016/j.scitotenv.2020.140511, 2020.

Brady, N. and Weil, R.: The nature and properties of soils, Pearson Education, Inc.0135133874, 2008.

Bryant, R. G.: Recent advances in our understanding of dust source emission processes, Progress in Physical Geography-Earth and Environment, 37, 397-421, 10.1177/0309133313479391, 2013.

Burezq, H.: Combating wind erosion through soil stabilization under simulated wind flow condition - Case of Kuwait, International Soil and Water Conservation Research, 8, 154-163, 10.1016/j.iswcr.2020.03.001, 2020.

Chang, A. C., Warneke, J. E., Page, A. L., and Lund, L. J.: Accumulation of Heavy Metals in Sewage Sludge-Treated Soils, Journal of Environmental Quality, 13, 87-91, https://doi.org/10.2134/jeq1984.00472425001300010016x, 1984.

Cheng, I., Xu, X., and Zhang, L.: Overview of receptor-based source apportionment studies for speciated atmospheric mercury, Atmospheric Chemistry and Physics, 15, 7877-7895, 10.5194/acp-15-7877-2015, 2015.

Ding, R. Q., Li, J. P., Wang, S. G., and Ren, F. M.: Decadal change of the spring dust storm in northwest China and the associated atmospheric circulation, Geophysical Research Letters, 32, 10.1029/2004gl021561, 2005.

DoE, U.: The risk assessment information system (RAIS), Argonne, IL: US Department of Energy's Oak Ridge Operations Office (ORO), 2011.

EPA, A.: Risk assessment guidance for superfund. Volume I: human health evaluation manual (part a), EPA/540/1-89/002, 1989.

Evan, A. T., Flamant, C., Fiedler, S., and Doherty, O.: An analysis of aeolian dust in climate models, Geophysical Research Letters, 41, 5996-6001, 10.1002/2014gl060545, 2014.

Fu, Q., Zhuang, G., Li, J., Huang, K., Wang, Q., Zhang, R., Fu, J., Lu, T., Chen, M., Wang, Q., Chen, Y., Xu, C., and Hou, B.: Source, long-range transport, and characteristics of a heavy dust pollution event in Shanghai, Journal of Geophysical Research: Atmospheres, 115, https://doi.org/10.1029/2009JD013208, 2010.

Fu, X., Wang, S. X., Cheng, Z., Xing, J., Zhao, B., Wang, J. D., and Hao, J. M.: Source, transport and impacts of a heavy dust event in the Yangtze River Delta, China, in 2011, Atmospheric Chemistry and Physics, 14, 1239-1254, 10.5194/acp-14-1239-2014, 2014.

Gholizadeh, A., Taghavi, M., Moslem, A., Neshat, A. A., Najafi, M. L., Alahabadi, A., Ahmadi, E., Asour, A. A., Rezaei, H., and Gholami, S.: Ecological and health risk assessment of exposure to atmospheric heavy metals, Ecotoxicology and environmental safety, 184, 109622, 2019a.

Gholizadeh, A., Taghavi, M., Moslem, A., Neshat, A. A., Lari Najafi, M., Alahabadi, A., Ahmadi, E., Ebrahimi aval, H., Asour, A. A., Rezaei, H., Gholami, S., and Miri, M.: Ecological and health risk assessment of exposure to atmospheric heavy metals, Ecotoxicology and Environmental Safety, 184, 109622, https://doi.org/10.1016/j.ecoenv.2019.109622, 2019b.

Gillette, D. and Goodwin, P. A.: Microscale transport of sand-sized soil aggregates eroded by wind, Journal of Geophysical Research, 79, 4080-4084, 10.1029/JC079i027p04080, 1974.

Griggs, D. J. and Noguer, M.: Climate change 2001: the scientific basis. Contribution of working group I to the third assessment report of the intergovernmental panel on climate change, Weather, 57, 267-269, 2002.

Grini, A. and Zender, C. S.: Roles of saltation, sandblasting, and wind speed variability on mineral dust aerosol size distribution during the Puerto Rican Dust Experiment (PRIDE), Journal of Geophysical Research-Atmospheres, 109, 10.1029/2003jd004233, 2004.

Grini, A., Zender, C. S., and Colarco, P. R.: Saltation Sandblasting behavior during mineral dust aerosol production, Geophysical Research Letters, 29, 10.1029/2002gl015248, 2002.

Guenther, A. B., Jiang, X., Heald, C. L., Sakulyanontvittaya, T., Duhl, T., Emmons, L. K., and Wang, X.: The Model of Emissions of Gases and Aerosols from Nature version 2.1 (MEGAN2.1): an extended and updated framework for modeling biogenic emissions, Geoscientific Model Development, 5, 1471-1492, 10.5194/gmd-5-1471-2012, 2012.

Gunawardana, C., Goonetilleke, A., Egodawatta, P., Dawes, L., and Kokot, S.: Source characterisation of road dust based on chemical and mineralogical composition, Chemosphere, 87, 163-170, 10.1016/j.chemosphere.2011.12.012, 2012.

Ho, K. F., Lee, S. C., Chow, J. C., and Watson, J. G.: Characterization of PM10 and PM2.5 source profiles for fugitive dust in Hong Kong, Atmospheric Environment, 37, 1023-1032, 10.1016/s1352-2310(02)01028-2, 2003.

Huang, K., Zhuang, G. S., Li, J. A., Wang, Q. Z., Sun, Y. L., Lin, Y. F., and Fu, J. S.: Mixing

of Asian dust with pollution aerosol and the transformation of aerosol components during the dust storm over China in spring 2007, Journal of Geophysical Research-Atmospheres, 115, 10.1029/2009jd013145, 2010.

Huebert, B. J., Bates, T., Russell, P. B., Shi, G. Y., Kim, Y. J., Kawamura, K., Carmichael, G., and Nakajima, T.: An overview of ACE-Asia: Strategies for quantifying the relationships between Asian aerosols and their climatic impacts, Journal of Geophysical Research-Atmospheres, 108, 10.1029/2003jd003550, 2003.

Huneeus, N., Schulz, M., Balkanski, Y., Griesfeller, J., Prospero, J., Kinne, S., Bauer, S., Boucher, O., Chin, M., Dentener, F., Diehl, T., Easter, R., Fillmore, D., Ghan, S., Ginoux, P., Grini, A., Horowitz, L., Koch, D., Krol, M. C., Landing, W., Liu, X., Mahowald, N., Miller, R., Morcrette, J. J., Myhre, G., Penner, J., Perlwitz, J., Stier, P., Takemura, T., and Zender, C. S.: Global dust model intercomparison in AeroCom phase I, Atmospheric Chemistry and Physics, 11, 7781-7816, 10.5194/acp-11-7781-2011, 2011.

Ikegami, M., Yoneda, M., Tsuji, T., Bannai, O., and Morisawa, S.: Effect of Particle Size on Risk Assessment of Direct Soil Ingestion and Metals Adhered to Children's Hands at Playgrounds, Risk Analysis, 34, 1677-1687, 10.1111/risa.12215, 2014.

Kaufman, Y. J., Tanre, D., and Boucher, O.: A satellite view of aerosols in the climate system, Nature, 419, 215-223, 10.1038/nature01091, 2002.

Kettler, T. A., Doran, J. W., and Gilbert, T. L.: Simplified Method for Soil Particle-Size Determination to Accompany Soil-Quality Analyses, Soil Science Society of America Journal, 65, 849-852, https://doi.org/10.2136/sssaj2001.653849x, 2001.

Kok, J. F., Ward, D. S., Mahowald, N. M., and Evan, A. T.: Global and regional importance of the direct dust-climate feedback, Nature Communications, 9, 10.1038/s41467-017-02620-y, 2018.

Kok, J. F., Storelvmo, T., Karydis, V. A., Adebiyi, A. A., Mahowald, N. M., Evan, A. T., He, C., and Leung, D. M.: Mineral dust aerosol impacts on global climate and climate change, Nature Reviews Earth & Environment, 10.1038/s43017-022-00379-5, 2023.

Lafon, S., Alfaro, S. C., Chevaillier, S., and Rajot, J. L.: A new generator for mineral dust aerosol production from soil samples in the laboratory: GAMEL, Aeolian Research, 15, 319-334, https://doi.org/10.1016/j.aeolia.2014.04.004, 2014.

Lafon, S., Sokolik, I. N., Rajot, J. L., Caquineau, S., and Gaudichet, A.: Characterization of iron oxides in mineral dust aerosols: Implications for light absorption, Journal of Geophysical Research-Atmospheres, 111, 10.1029/2005jd007016, 2006.

Li, L., Huang, Z. X., Dong, J. G., Li, M., Gao, W., Nian, H. Q., Fu, Z., Zhang, G. H., Bi, X. H., Cheng, P., and Zhou, Z.: Real time bipolar time-of-flight mass spectrometer for analyzing single aerosol particles, International Journal of Mass Spectrometry, 303, 118-124, 10.1016/j.ijms.2011.01.017, 2011.

Liu, Q., Liu, X., Liu, T., Kang, Y., Chen, Y., Li, J., and Zhang, H.: Seasonal variation in particle contribution and aerosol types in Shanghai based on satellite data from MODIS and CALIOP, Particuology, 51, 18-25, https://doi.org/10.1016/j.partic.2019.10.001, 2020.

Liu, Q., Wang, Y., Kuang, Z., Fang, S., Chen, Y., Kang, Y., Zhang, H., Wang, D., and Fu, Y.: Vertical distributions of aerosol optical properties during haze and floating dust weather in Shanghai, Journal of Meteorological Research, 30, 598-613, 10.1007/s13351-016-5092-4, 2016.

Liu, X. D., Yin, Z. Y., Zhang, X. Y., and Yang, X. C.: Analyses of the spring dust storm frequency of northern China in relation to antecedent and concurrent wind, precipitation, vegetation,

644 and soil moisture conditions, Journal of Geophysical Research-Atmospheres, 109,
645 10.1029/2004jd004615, 2004.

646 Lowenthal, D. H., Watson, J. G., Koracin, D., Chen, L.-W. A., Dubois, D., Vellore, R., Kumar,
647 N., Knipping, E. M., Wheeler, N., and Craig, K.: Evaluation of regional-scale receptor modeling,
648 Journal of the Air & Waste Management Association, 60, 26-42, 2010.

649 Luo, X.-S., Ding, J., Xu, B., Wang, Y.-J., Li, H.-B., and Yu, S.: Incorporating bioaccessibility
650 into human health risk assessments of heavy metals in urban park soils, Science of the Total
651 Environment, 424, 88-96, 2012.

652 Lv, M., Hu, A., Chen, J., and Wan, B.: Evolution, Transport Characteristics, and Potential
653 Source Regions of PM2.5 and O3 Pollution in a Coastal City of China during 2015–2020,
654 Atmosphere, 12, 1282, 2021.

655 Middleton, N., Tozer, P., and Tozer, B.: Sand and dust storms: underrated natural hazards,
656 Disasters, 43, 390-409, 10.1111/disa.12320, 2019.

657 Miller, M. S., Friedlander, S. K., and Hidy, G. M.: A chemical element balance for the Pasadena
658 aerosol, Journal of Colloid and Interface Science, 39, 165-176, https://doi.org/10.1016/0021-
659 9797(72)90152-X, 1972.

660 Moya, J., Phillips, L., Schuda, L., Wood, P., Diaz, A., Lee, R., Clickner, R., Birch, R., Adjei,
661 N., and Blood, P.: Exposure factors handbook: 2011 edition, US Environmental Protection Agency,
662 2011.

663 Naderizadeh, Z., Khademi, H., and Ayoubi, S.: Biomonitoring of atmospheric heavy metals
664 pollution using dust deposited on date palm leaves in southwestern Iran, Atmósfera, 29, 141-155,
665 10.20937/ATM.2016.29.02.04, 2016.

666 Parajuli, S. P., Zobeck, T. M., Kocurek, G., Yang, Z. L., and Stenchikov, G. L.: New insights
667 into the wind-dust relationship in sandblasting and direct aerodynamic entrainment from wind
668 tunnel experiments, Journal of Geophysical Research-Atmospheres, 121, 1776-1792,
669 10.1002/2015jd024424, 2016.

670 Perlwitz, J. P., Pérez García-Pando, C., and Miller, R. L.: Predicting the mineral composition
671 of dust aerosols – Part 1: Representing key processes, Atmos. Chem. Phys., 15, 11593-11627,
672 10.5194/acp-15-11593-2015, 2015.

673 Pongkiatkul, P. and Kim Oanh, N. T.: Assessment of potential long-range transport of
674 particulate air pollution using trajectory modeling and monitoring data, Atmospheric Research, 85,
675 3-17, https://doi.org/10.1016/j.atmosres.2006.10.003, 2007.

676 Prospero, J. M., Ginoux, P., Torres, O., Nicholson, S. E., and Gill, T. E.: Environmental
677 characterization of global sources of atmospheric soil dust identified with the Nimbus 7 Total Ozone
678 Mapping Spectrometer (TOMS) absorbing aerosol product, Reviews of geophysics, 40, 2-1-2-31,
679 2002.

680 Samiksha, S., Raman, R. S., Nirmalkar, J., Kumar, S., and Sirvaiya, R.: PM10 and PM2. 5
681 chemical source profiles with optical attenuation and health risk indicators of paved and unpaved
682 road dust in Bhopal, India, Environmental Pollution, 222, 477-485, 2017.

683 Santos, J. M., Reis, N. C., Galvão, E. S., Silveira, A., Goulart, E. V., and Lima, A. T.: Source
684 apportionment of settleable particles in an impacted urban and industrialized region in Brazil,
685 Environmental Science and Pollution Research, 24, 22026-22039, 2017.

686 Shangguan, Y., Zhuang, X., Querol, X., Li, B., Moreno, N., Trechera, P., Sola, P. C., Uzu, G.,
687 and Li, J.: Characterization of deposited dust and its respirable fractions in underground coal mines:

Implications for oxidative potential-driving species and source apportionment, International Journal of Coal Geology, 258, 104017, https://doi.org/10.1016/j.coal.2022.104017, 2022.

Shao, Y. and Dong, C. H.: A review on East Asian dust storm climate, modelling and monitoring, Global and Planetary Change, 52, 1-22, 10.1016/j.gloplacha.2006.02.011, 2006.

Shao, Y. and Raupach, M. R.: Effect of saltation bombardment on the environment of dust by wind, Journal of Geophysical Research-Atmospheres, 98, 12719-12726, 10.1029/93jd00396, 1993.

Shao, Y. P., Klose, M., and Wyrwoll, K. H.: Recent global dust trend and connections to climate forcing, Journal of Geophysical Research-Atmospheres, 118, 11107-11118, 10.1002/jgrd.50836, 2013.

Shao, Y. P., Raupach, M. R., and Leys, J. F.: A model for predicting aeolian sand drift and dust entrainment on scales from paddock to region, Australian Journal of Soil Research, 34, 309-342, 10.1071/sr9960309, 1996.

Shi, J., Li, Z., Sun, Z., Han, X., Shi, Z., Xiang, F., and Ning, P.: Specific features of heavy metal pollutant residue in PM2. 5 and analysis of their damage level for human health in the urban air of Kunming, J. Saf. Environ, 18, 795-800, 2018.

Simon, H., Beck, L., Bhave, P. V., Divita, F., Hsu, Y., Luecken, D., Mobley, J. D., Pouliot, G. A., Reff, A., and Sarwar, G.: The development and uses of EPA's SPECIATE database, Atmospheric Pollution Research, 1, 196-206, 2010.

Sullivan, R., Guazzotti, S., Sodeman, D., and Prather, K.: Direct observations of the atmospheric processing of Asian mineral dust, Atmospheric Chemistry and Physics, 7, 1213-1236, 2007.

Sun, R., Wang, H., Ma, X., Chen, Y., Zhao, B., Qin, Y., Zhang, H., and Ye, W.: Aerosol optical properties and formation mechanism of a typical air pollution episode in Shanghai during different weather condition periods, Acta Scientiae Circumstantiae, 37, 814-823, 2017.

Tang, M. J., Cziczo, D. J., and Grassian, V. H.: Interactions of Water with Mineral Dust Aerosol: Water Adsorption, Hygroscopicity, Cloud Condensation, and Ice Nucleation, Chemical Reviews, 116, 4205-4259, 10.1021/acs.chemrev.5b00529, 2016.

Textor, C., Schulz, M., Guibert, S., Kinne, S., Balkanski, Y., Bauer, S., Berntsen, T., Berglen, T., Boucher, O., Chin, M., Dentener, F., Diehl, T., Easter, R., Feichter, H., Fillmore, D., Ghan, S., Ginoux, P., Gong, S., Kristjansson, J. E., Krol, M., Lauer, A., Lamarque, J. F., Liu, X., Montanaro, V., Myhre, G., Penner, J., Pitari, G., Reddy, S., Seland, O., Stier, P., Takemura, T., and Tie, X.: Analysis and quantification of the diversities of aerosol life cycles within AeroCom, Atmospheric Chemistry and Physics, 6, 1777-1813, 10.5194/acp-6-1777-2006, 2006.

Urrutia-Pereira, M., Rizzo, L. V., Staffeld, P. L., Chong-Neto, H. J., Viegi, G., and Sole, D.: Dust from the Sahara to the American Continent: Health impacts, Allergologia Et Immunopathologia, 49, 187-194, 10.15586/aei.v49i4.436, 2021.

Wang, L., Li, H., Zhang, W., Qi, J., Tian, H., Huang, K., Chen, D., and Guo, J.: Regional Pollution Characteristics of Heavy Metals in PM2.5, Research of Environmental Sciences, 34, 849-862, 2021.

Wu, F., Cheng, Y., Hu, T., Song, N., Zhang, F., Shi, Z., Hang Ho, S. S., Cao, J., and Zhang, D.: Saltation–Sandblasting Processes Driving Enrichment of Water-Soluble Salts in Mineral Dust, Environmental Science & Technology Letters, 2022.

Xia, Z., Fan, X., Huang, Z., Liu, Y., Yin, X., Ye, X., and Zheng, J.: Comparison of Domestic and Foreign PM$_{2.5}$ Source Profiles and Influence on Air Quality Simulation, Research of

Environmental Sciences, 30, 359-367, 2017.

Yang, Y. Q., Hou, Q., Zhou, C. H., Liu, H. L., Wang, Y. Q., and Niu, T.: Sand/dust storm processes in Northeast Asia and associated large-scale circulations, Atmospheric Chemistry and Physics, 8, 25-33, 10.5194/acp-8-25-2008, 2008.

Ying, Q., Feng, M., Song, D., Wu, L., Hu, J., Zhang, H., Kleeman, M. J., and Li, X.: Improve regional distribution and source apportionment of PM2. 5 trace elements in China using inventory-observation constrained emission factors, Science of the total environment, 624, 355-365, 2018.

Zhang, H. R. and Tripathi, N. K.: Geospatial hot spot analysis of lung cancer patients correlated to fine particulate matter (PM2.5) and industrial wind in Eastern Thailand, Journal of Cleaner Production, 170, 407-424, 10.1016/j.jclepro.2017.09.185, 2018.

Zhuang, G. S., Guo, J. H., Yuan, H., and Zhao, C. Y.: The compositions, sources, and size distribution of the dust storm from China in spring of 2000 and its impact on the global environment, Chinese Science Bulletin, 46, 895-901, 10.1007/bf02900460, 2001.